Vol. 44, No. 4 (2022) 608-624, DOI: 10.24874/ti.1318.06.22.10

Tribology in Industry

www.tribology.rs

RESEARCH

Studying the Temperature Characteristics of Oil at the Outlet From the K27-145 Turbocharger Rotor Bearing

Alexander V. Gritsenko[a,b], Vladimir D. Shepelev[b,*], Beibit K. Kaliyev[c]

[a]*Department of Machine-Tractor Fleet Operation, South Ural State Agrarian University, Troitsk, Russia,*
[b]*Department of Automobile Transport, South Ural State University, Chelyabinsk, Russia,*
[c]*Department of Mechanical Engineering, NLC "A. Baitursynov Kostanay Regional University", Kostanay, Kazakhstan.*

Keywords:

Turbocharging
Bearing
Turbocharger
Engine oil
Lubrication system

* Corresponding author:

Vladimir Shepelev
E-mail: shepelevvd@susu.ru

Received: 14 June 2022
Revised: 12 September 2022
Accepted: 4 October 2022

A B S T R A C T

Turbocharging is a promising solution for increasing the specific power of motor-and-tractor equipment, which allows increasing power up to 50%. At the same time, a significant growth of speed, load, and temperature modes leads to a significant increase in the number of failures and a decrease in reliability by 2–3 times. Theoretical and experimental studies established that the temperature of the bearing and oil at the turbocharger drain changes under the influence of the inlet oil temperature to the TCR bearing, the TCR rotor shaft speed, and the change in the oil pressure at the input to the TCR bearing. This allows setting the limits of the TCR bearing performance in extreme operating conditions. The installation of an autonomous TCR lubricating and braking device maintains the required reliability level and increases failure-free operation. The hydraulic accumulator installed in the lubrication system of the engine turbocharger regulars lubricates and cools the rotor bearings when the ICE crankshaft speed drops. The incorporation of a braking device reduces the rundown time of the rotor and thereby prevents oil starvation and dry friction of the rotor bearing. The combined use of the hydraulic accumulator and the braking device minimizes the risk of dry friction and accidental failure of the turbocharger. We proved that the braking device of the TCR rotor built into the intake system of an ICE with the calculated design parameters reduces the rotor rundown time by 30–35%. This reduces the dimensions and operating time of the hydraulic accumulator and simultaneously eliminates surges in the compressor section of the TCR and any breakage of its parts. In these conditions, it is relevant to develop independent systems to lubricate the TCR bearings and replenish them using built-in hydraulic accumulators during start-up, significant loads at minimum crankshaft speeds, and engine stalling.

© 2022 Published by Faculty of Engineering

1. INTRODUCTION

The automotive industry aims at a constant increase in the operating efficiency of road transport, in particular, increasing the power characteristics of engines while reducing fuel consumption and harmful emissions [1-3]. There are several ways to increase engine power and flexibility, however turbocharging is the most effective way. Turbocharging has some disadvantages, such as delays [4], failures [5-7], noise and vibration [8].

Turbocharger lifetimes are significantly shorter than engine lifetimes, they require high quality engine oil and a defective TCR can damage the engine itself [9-11].

A TCR consists of a radial compressor and an exhaust gas-driven turbine. The TCR is a complex heat transfer system and consists of three different solid parts (compressor, turbine, and bearing body). The compressor captures fresh air, the turbine captures exhaust gases, and the bearing housing captures the lubricating oil and water. All these working fluids interact with each other and with the surrounding air using heat transfer mechanisms. Heat transfer from the turbine gases to the lubricating oil and the compressor should be limited since high oil temperatures can degrade the lubricant, resulting in bearing failure. Heat transfer between the lubricating oil and the compressor affects the compressor's performance. The bearing housing is also designed to limit conductive heat transfer through the structure [12].

The experimental studies carried out by Alaviyoun and Ziabasharhagh [13] showed that the maximum temperature comes from the outer turbine surface. The temperature of the turbine surface is very sensitive to the gas temperature at the turbine outlet and to changes in the mass flow. Forced convection heat transfer is five times higher than the measured free convection heat. Heat transfer to the compressor results in a reduction in efficiency.

Basir et al. [14] used thermocouples and an infrared camera to study the temperature distribution of the TCR housing in engines. They found that the temperature of the bearing housing near the turbine housing is higher than the area adjacent to the compressor body. Radiative heat transfer from the compressor and turbine bodies also affects the housing temperature. Heat distribution in TCR is uneven, which causes high thermal stress on the TCR body.

Apart from lubrication, oil is also used for cooling and cleaning. Taylor et al. [15] investigated the influence of lubricants on energy efficiency. The use of lubricants with different viscosities affects the friction mean effective pressure of the engine. The modification of parts and equipment in machines and the use of lubricants with reduced viscosity will not only extend the life of the vehicle itself and reduce fuel consumption, but also reduce emissions.

Dellis et al. [5] analyzed the factors affecting TCR wear and damage in their review article on TCR lubrication systems. The researchers revealed that most TCR failures (up to 50%) are caused by lubrication problems (30% are caused by a delay in the lubricant flow into the TCR and 20% by a lack of sufficient lubrication). In further research [16,17], the author studied cavitation in the lubrication of piston rings and its dependence on the composition of the lubricant.

Each TCR element was updated to improve its reliability and performance. Failures can occur not only due to oil contamination but also at high bearing system temperatures. The model developed by Gil et al. [18] allows the study of the maximum temperature at various points of the bearing system of an automobile TCR and the temperature rise of the lubrication channels and the central body. This model allows to evaluate the thermal damage of the entire TCR, which affects the temperature of the working fluid, which ultimately affects the performance of the engine itself.

During hot engine stops, the lack of the oil flow inside the TCR leads to the combustion of oil trapped in the bearings and the formation of coke, which clogs the bearings, resulting in a decrease in compressor efficiency and shaft damage [19]. Serrano et al. [20] developed a methodology to model several combinations of strategies for cooling the central housing of an ICE TCR and find the optimal one to minimize additional energy consumption.

Sandoval et al. [22] investigated the dependence of the temperature and pressure of TCR lubricating oil on the vibration amplitude of its components.

Hadryś et al. [23] carried out wear tests on the TCR shaft surface and found that various factors influence wear: engine load, TCR and lubricating oil temperature, lubricating oil quality, the replacement of lubricating oil, lubricating oil filtration quality, air filtration quality, and tightness and completeness of the intake and exhaust systems. The maximum wear of the TCR shaft surface occurred when high viscosity, contaminated oil is used.

The mechanical efficiency of TCRs is mainly influenced by the lubrication system; therefore, to reduce the loss of performance, Novotný et al. [24] developed a strategy allowing an increase in the performance of the TCR lubrication system. This strategy will be used by the authors to develop a new design of the TCR thrust bearing to reduce mechanical losses in the lubrication system.

Chuepeng and Saipom [25] tested TCRs with two types of lubricating oils at different inlet temperatures. The results showed that higher inlet temperatures lead to an increase in TCR efficiency, i.e., heat treatment of the lubricant is needed for the operation of the TCR at low loads.

The mechanical efficiency of turbochargers is mainly affected by the lubrication system; therefore, to reduce the TCR performance losses, Novotný et.al [26] developed a solution strategy to improve the performance of the TCR lubrication system. This strategy will be used to develop a new TCR thrust bearing configuration to reduce mechanical losses in the lubrication system.

The TCR operation fails for such reasons as bearings wear and shaft cracks [27], so the TCR configuration should be sufficiently reliable and resistant to negative impacts. Mutra et al. [28] developed a numerical simulation platform to study the influence of the bearing parameters and the load factor on the amount of exhaust gases and the rotor speed. To predict the optimal bearing parameters, a surrogate model was used combined with a trained backpropagation neural network model, which turned out to be more efficient than other models. The study [29] developed a methodology to predict the bearing coefficients, and the study [27] investigated and modelled the stability of the TCR rotor system using a neural network model and proposed the optimal design of the bearing foil parameters.

The TCR rotor-bearing system experiences significant thermal loads and should be subject to frequent fault monitoring [28]. The study [28] revealed patterns of rotor failures in start-up and stop conditions. The proposed approach allows determining the optimal clearance and type of lubrication depending on temperature changes in the system.

In our paper, we study the temperature characteristics of the lubricating oil at the outlet of the K27-145 TCR rotor bearing at various operating parameters of the TCR lubrication system. The most informative method is that based on the analysis of the characteristics of engine rundown, a TCR or any other triboconjugation operating with liquid lubrication [30]. We identify the relationship between the oil outlet temperature and the operating parameters of the TCR lubrication system.

This study proposes to use an adaptive external autonomous lubrication system to prevent dry friction of the TCR rotor bearing. The autonomous lubrication system sets the range of the oil pressure before the bearing from 0 to 0.5MPa and the oil temperature up to 130ºC. The use of a hydraulic accumulator and a braking device in the TCR lubrication system prevents oil starvation of the rotor bearing, which was established experimentally on the developed rig. Such tests have not been previously considered in the literature, which proves the practical importance of this study.

2. MATERIALS AND METHODS

Let us consider the process of lubricating a TCR bearing and its thermal conditions. To this end, the heat balance for the TCR body is Eq. (1):

$$C_m \cdot m_s \frac{dT_s}{dt} = -a_1 \cdot A_1 (T_s - T_b) - \\ - a_2 \cdot A_2 (T_s - T_0) + \frac{N_g \left(sign(t)+1\right)}{2} \quad (1)$$

where C_m is the specific heat capacity of the TCR body, depending on the material used, J/(kg·K); m_s is the mass of the TCR housing section, kg; T_s is the temperature of the TCR housing section, ºC ; t is the time interval, s; a_1 is the coefficient of heat transfer from the TCR housing to the bearing, W/(m²·K); A_1 is the total surface area of heat transfer from the TCR housing section to the bearing unit, m²; T_b is the temperature of the TCR bearing, ºC ; a_2 is the coefficient of heat transfer from the TCR housing section to the surrounding atmosphere, W/(m²·K); T_0 is the air temperature at which the measurements are carried out, ºC ; N_g is the power of the gas flow transmitted to the TCR housing section, W.

For the housing section of the TCR bearing, the heat balance can be written in differential form:

$$C_m \cdot m_b \frac{dT_b}{dt} = -a_1 \cdot A_1 (T_s - T_b) - \\ - a_3 \cdot A_3 (T_b - T_0) + N_c(t) + \frac{N_p \left(sign(t - t_{cut}) + 1\right)}{2} \quad (2)$$

where m_b is the mass of housing section of the TCR bearing, kg; a_3 is the coefficient of heat transfer from the housing section of the TCR bearing to the surrounding atmosphere, W/(m²·K); A_3 is the total surface area of heat transfer from the housing section of the TCR bearing to the surrounding atmosphere, m²; $N_c(t)$ is the power of the heat flow arising from the forces of viscous friction in the TCR bearing after stopping the ICE, W; N_p is the power of the heat flow additionally removed when a hydraulic accumulator is installed in the standard lubrication system, W; t_{cut} is the time interval from the moment of cutting off the ICE, s.

The Eq. (2) of the rotational motion of the TCR rotor in differential form is:

$$J_m \frac{d\omega_r}{dt} = k_{T1} P_w - k_{T2} \omega_r + k_{T3} h_f - k_{T4} P_{TCR} \quad (3)$$

where J_m is the TCR moment of inertia reduced to the rotor, N·m·s²; ω_r is the angular speed of the TCR rotor, rad/s; k_{T1}, k_{T2}, k_{T3}, k_{T4} are constant coefficients, determined when taking the objective parameters of the studied TCR; P_w is the pressure before the TCR turbine wheel transmitted from the exhaust system, Pa; h_f is the stroke of the fuel supply working body, m; P_{TCR} is the pressure created after the TCR compressor wheel, Pa.

When stopping the ICE, $h_f \to 0$, and when the ICE is completely stopped, $h_f = 0$. As a result, in Eq. (3), one term vanishes. The Eq. (4) can be written for the TCR inlet pipe:

$$k_{C1} P_{TCR} = \omega_r - k_{C2} \omega_{as} \quad (4)$$

where k_{C1} and k_{C2} are constant coefficients determined by the parameters of the TCR; ω_{as} is the angular speed of the ICE crankshaft.

When the ICE is braking, ω_{as} tends to vanish, and when the engine is completely stopped, $\omega_{as} = 0$. As a result, in Eq. (4), one term vanishes. The following condition can be written for the outlet pipe:

$$k_{op1} P_w = \omega_{as} + k_{op2} \cdot P_{TCR} - k_{op3} \cdot h_f \quad (5)$$

where k_{op1}, k_{op2} and k_{op3} are constant coefficients determined by the parameters of the TCR.

When the ICE is completely stopped, $\omega_{as} = 0$ and $h_f = 0$. Taking this into account, several terms in Eq. (5) vanish. When the lubrication system is fed by an external independent lubrication system, the Eq. (5) can be written as:

$$J_{rm} \frac{d\omega_r}{dt} = M_t - k_r \cdot \omega_r - M_s \quad (6)$$

where J_{rm} is the reduced moment of inertia of the drive motor spindle of the oil pump drive, N·m·s²; M_t is the torque taken from the electric motor shaft of the oil pump drive, N·m; k_r is the coefficient of resistance of the rotary motion of the rotor caused by the viscous friction of oil, N·m·s; M_s is the moment of resistance on the motor spindle shaft of the oil pump drive, N·m.

The moment of resistance on the motor spindle shaft of the oil pump drive can be determined from the Eq. (7):

$$M_s = k_{e1} \cdot P_{ls} \quad (7)$$

where k_{e1} is the experimentally determined coefficient; P_{ls} is the pressure created by the independent lubrication system, Pa.

When the pressure in the independent lubrication system reaches the maximum and the bypass valve is activated, the equation can be written as follows:

$$m_{bv} \frac{d^2 x}{dt_v^2} = A_v \cdot P_{ls} - k_{bv} \frac{dx}{dt_v} - c_{bv}(x - x_0) \quad (8)$$

where m_{bv} is the total mass of the bypass valve, kg; x is the current movement of the bypass valve, m; t_v is the interval of the bypass valve operation, s; A_v is the total valve surface area, m²; k_{bv} is the coefficient characterizing the resistance to movement of the bypass valve from the part of the viscous friction forces, N·s/m; c_{bv} is the stiffness of the counter spring in the bypass valve, N/m; x_0 is the tension of the bypass valve spring, m.

Eqs. (1-8) were combined into a system and solved in the Simulink program. During the calculation, the initial parameter was the temperature of the exhaust gases ($t_{exhaust}$) when the ICE was stopped (according to several studies, the exhaust temperature determines the temperature of the bearing and the oil passing through it). Out of all the possible options, we selected three operating temperatures, which make up to 90% of the ICE operating modes: 600ºC is the temperature for using the ICE at full load (nominal operating mode); 420ºC is the temperature of an average load; 300ºC is the temperature typical for idling.

The results are given for the theoretical dependences of the temperature of the housing section and the bearing of the TCR with a standard lubrication system (Fig. 1) and an external independent lubrication system (Fig. 2) (the calculations were made in the Simulink program).

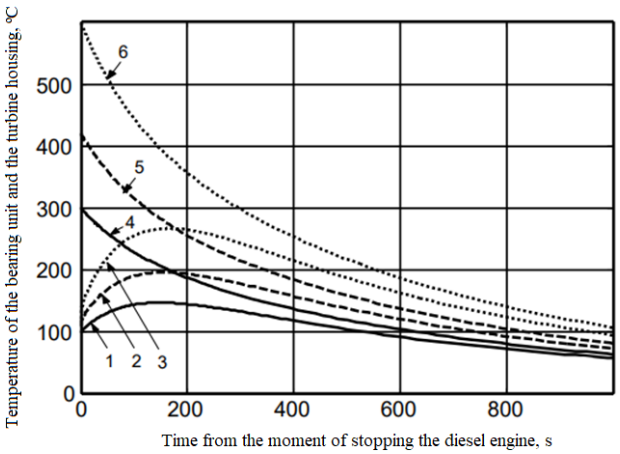

Fig. 1. The theoretical dependence of the temperature of the TCR housing section and the bearing on the time from the moment of stopping a KAMAZ diesel engine with a standard lubrication system: 1, 2 and 3 are the temperatures of the TCR bearings when the calculations were started from 98ºC, 108ºC and 120ºC, respectively; 4, 5, and 6 are the temperatures of the TCR housing section when the calculations were started from 98ºC, 108ºC and 120ºC, respectively.

Fig. 1 shows that when a standard lubrication system is used, after stopping the ICE, the temperature of the bearings begins to grow significantly. For the initial low temperatures of 98ºC and 108ºC, the maximum temperature rise is 147ºC and 200ºC, respectively. For example, the maximum growth is observed at the initial bearing temperature of 120ºC and is $\Delta t_{bearing}$ = 150ºC. The resulting $t_{bearing}$=270ºC already exceeds the oil flash point, which is 230–240ºC for modern high-quality oils. A significant temperature rise leads to overheating of the oil in the bearing clearance and its subsequent coking.

Fig. 2 shows that when an independent external lubrication system is used, there is no temperature rise over the entire time period. From 0 to 1,000 s, the temperature of the bearings does not rise above 120ºC, which indicates that the lubrication of the TCR bearing is improved when it is supplied from an external lubrication system.

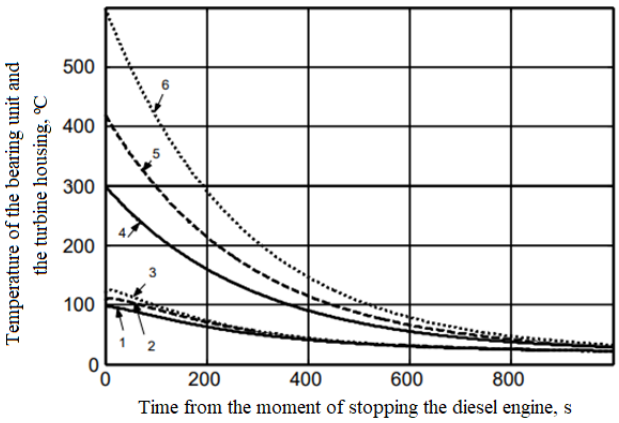

Fig. 2. The theoretical dependence of the temperature of the TCR housing section and the bearing on the time from the moment of stopping a KAMAZ diesel engine with an independent lubrication system: 1, 2 and 3 are the temperatures of the TCR bearings when the calculations were started from 98ºC, 108ºC and 120ºC, respectively; 4, 5, and 6 are the temperatures of the TCR housing section when the calculations were started from 98ºC, 108ºC and 120ºC, respectively.

We use the data obtained from [1,31-33] when assessing the temperature of the TCR bearing and the oil in the bearing clearance. We consider the dependencies of the TCR bearing temperature on time when the ICE is stopped with a standard lubrication system and with an external independent lubrication system (Fig. 3).

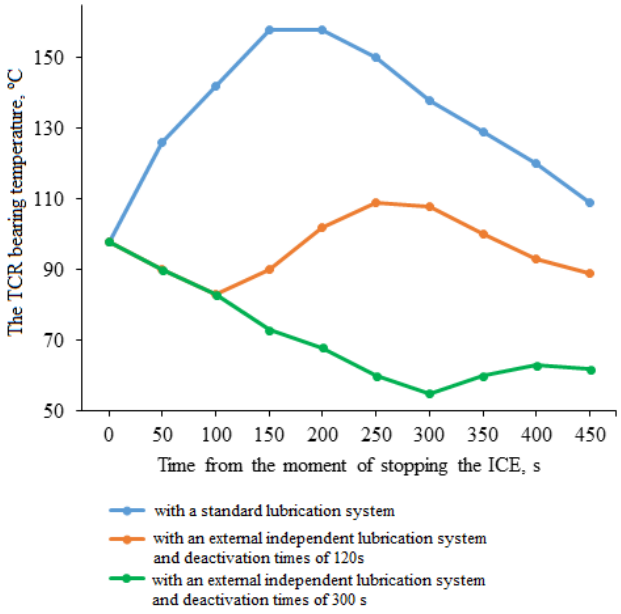

Fig. 3. The theoretical dependence of the TCR bearing temperature on time when stopping the ICE (the value of the ICE crankshaft speed was maintained at 600 rpm). Operation on mineral oil.

Fig. 3 shows that when the ICE is stopped with a standard lubrication system, the temperature of the TCR bearing begins to increase sharply from the first second and reaches a maximum value of 160ºC after 180 seconds. Under these extreme conditions, the oil temperature in the TCR bearing clearance also rises and the circulation of oil through the bearing stops, which significantly complicates the removal of heat from the friction zone. However, when an external independent lubrication system is used and the ICE is stopped, the situation improves. After 60 seconds, the maximum temperature of the TCR bearing is only 130ºC. When the deactivation time is 300 seconds, the maximum temperature of the TCR bearing does not rise above 70ºC, which indicates the most favorable operating mode of the TCR bearing.

This study considers the part of the bearing installed at the end of the turbine wheel, since in this part, the turbocharger is under significant thermal loads and oil coking during overheating is highly probable at this point.

A test rig and an autonomous lubrication system for the TCR bearing were designed to determine the exact volume of oil supplied to the bearing. The temperature of the inlet oil supplied into the bearing was also set very precisely and controlled during the experiment. The test conditions were close to real. The oil in the test rig during the study was used according to the GOST requirements and the regulations for the operation of turbocharged propulsion systems. The oil was replaced simultaneously in the entire system with the removal of lubricants in hard-to-reach places. At the same time, the filter element was replaced and the lines were partially disassembled.

The situation is similar in Fig. 4, showing improved thermal conditions of the TCR bearing lubrication; a decrease in the temperature of the TCR rotor bearing when an external independent lubrication system is used, and its deactivation time is increased. The authors consider the optimal time of continuous lubrication of the TCR bearing from an external lubrication system, taking into account that the bearing temperature was at a significantly low level.

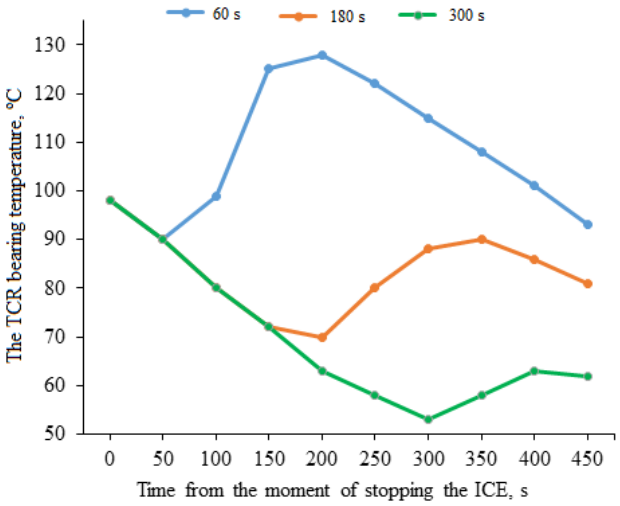

Fig. 4. The theoretical dependence of the TCR bearing temperature on time when stopping the ICE (the value of the ICE crankshaft speed was maintained at 600 rpm) with an external independent lubrication system and different deactivation times. Operation on synthetic oil.

Let us consider the option of stopping the ICE at the initial ICE crankshaft speed of 1,300 rpm (Fig. 5). We can see that the bearing temperature increased significantly compared to when the ICE crankshaft speed is 600 rpm.

Fig. 5 shows that when stopping the engine when a standard lubrication system is used, the highest temperature conditions are observed for the TCR bearing. The maximum bearing temperature

rises to 200–205ºC. The use of an external independent lubrication system can significantly reduce the temperature of the TCR bearings. For example, with an external lubrication system and a deactivation time of 120 seconds, the bearing temperature does not exceed 134ºC.

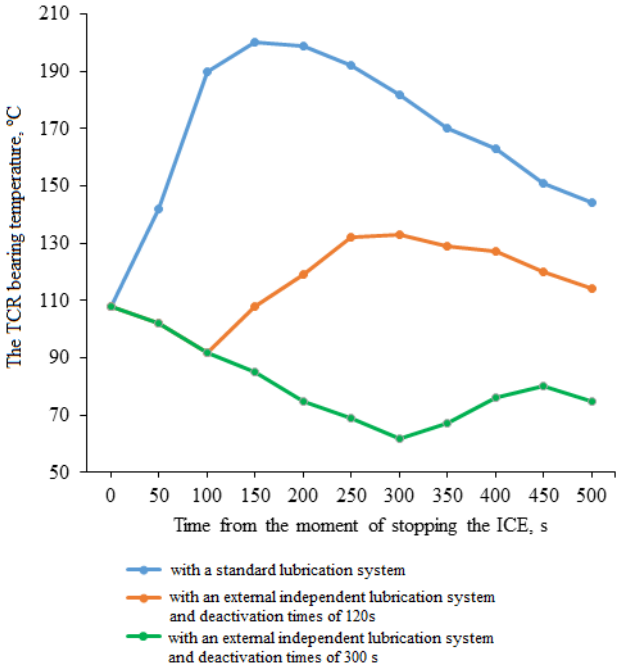

Fig. 5. The theoretical dependence of the TCR bearing temperature on time when stopping the ICE (the value of the ICE crankshaft speed was maintained at 1300 rpm) with an external independent lubrication system and different deactivation times, operation on mineral oil.

The use of synthetic oil reduces the maximum temperature of the TCR bearing by 3–6ºC compared to the use of mineral oils (Fig. 6).

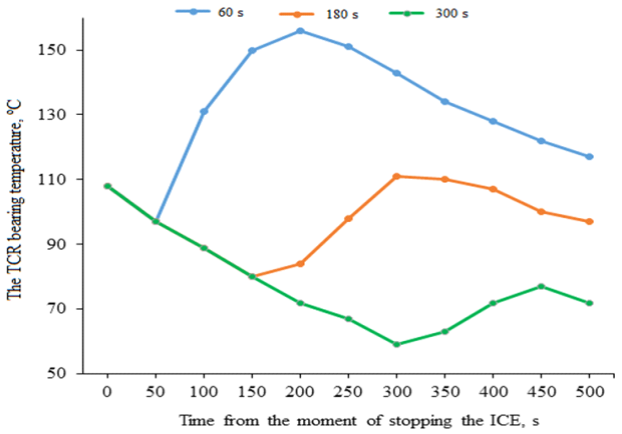

Fig. 6. The theoretical dependence of the TCR bearing temperature on time when stopping the ICE (the value of the ICE crankshaft speed was maintained at 1300 rpm) with an external independent lubrication system and different deactivation times, operation on synthetic oil.

We conclude that it is preferable to use synthetic oils, which are more resistant to temperature changes, for lubricating TCR bearings.

The study of the most loaded operating modes of the TCR bearing is of maximum interest. Such a mode corresponds to the nominal ICE crankshaft speed (Fig.7).

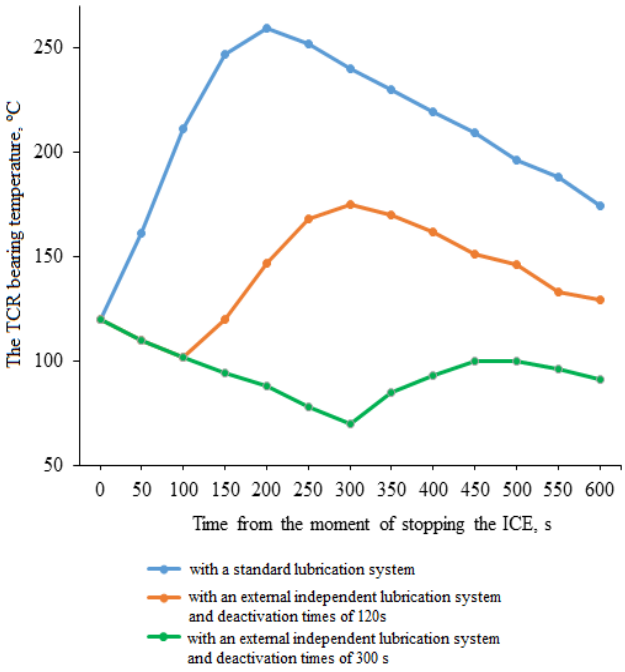

Fig. 7. The theoretical dependence of the TCR bearing temperature on time when stopping the ICE (the value of the ICE crankshaft speed was maintained at 2,200 rpm), operation on mineral oil.

Fig. 7 shows the highest temperature of the TCR bearing is observed when a standard lubrication system is used. The maximum temperature is observed about 200 seconds after stopping the ICE (256ºC). This temperature maximum lies in the flash point zone of modern oils and is dangerous because the inner layers of oil can cause coking in the TCR bearing clearance and its channels. However, when an external independent lubrication system is used and is deactivated in 120 seconds, the temperature of the TCR bearing decreases to a value below 175ºC.

A comparison of the data shown in Figs. 7 and 8 suggests that more favorable lubrication conditions are observed when synthetic oils are used, the average temperature difference was 2–6ºC.

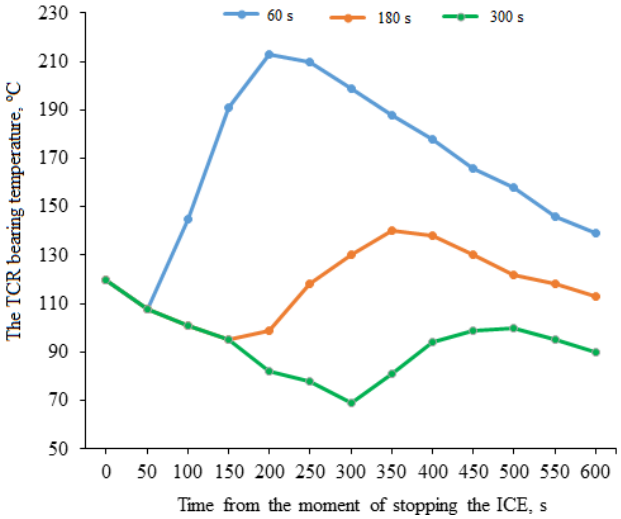

Fig. 8. The theoretical dependence of the TCR bearing temperature on time when stopping the ICE (the value of the ICE crankshaft speed was maintained at 2200 rpm) with an external independent lubrication system and different deactivation times, operation on synthetic oil.

Denisov et al. [32] determined the dependence of the bearing temperature on the exhaust gas temperature and the operating time of the independent lubrication system after stopping the diesel engine (Fig. 9).

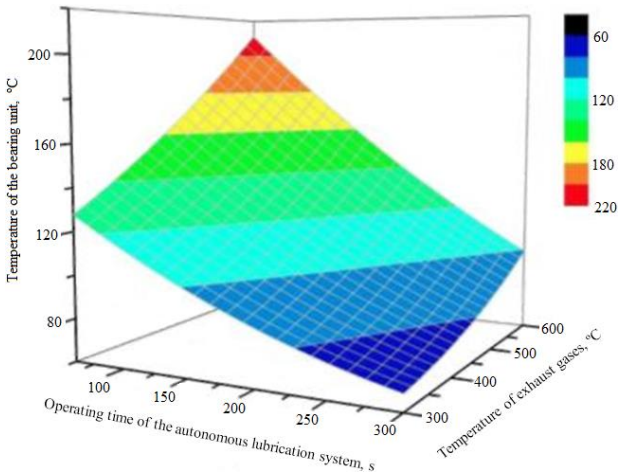

Fig. 9. The dependence of the TCR bearing temperature on the exhaust gas temperature and the operating time of an independent lubrication system after stopping the diesel engine.

Fig. 9 shows that at an exhaust gas temperature of 600ºC and the minimum operating time of the independent lubrication system reaches a maximum value of about 210ºC. An increase in the operating time of the independent lubrication system and a decrease in the exhaust gas temperature leads to a decrease in temperature of bearing.

By systematizing the above data [1,31-33] we obtained theoretical dependencies revealing the relationship between the temperature of the TCR bearing with the parameters of the exhaust system and the external independent lubrication system of the ICE, provided that the TCR lubrication system operates on:

- mineral oil:

$$T_{b\_m} = 118.875 - 43.333 \cdot t_{ex} + 28.833 \cdot t_p - \\ -13 \cdot t_{ex} \cdot t_p + 6.833 \cdot t_{ex}^2 + 3.5 \cdot t_p^2 \quad (9)$$

where T_{b_m} is the temperature of the bearing unit with mineral oil, ºC; t_{ex} is the operating period of the external independent lubrication system, s; t_p is the average temperature at the ICE outlet, ºC.

- synthetic oil:

$$T_{b\_s} = 114.875 + 43 \cdot t_{ex} + 28.833 \cdot t_p - \\ -13 \cdot t_{ex} \cdot t_p + 4.633 \cdot t_{ex}^2 + 4.833 \cdot t_p^2 \quad (10)$$

where T_{b_s} is the temperature of the bearing unit with synthetic oil, ºC.

Eqs. (9–10) show that the best conditions for lubricating the TCR bearing and removing excess temperature are provided when an external independent lubrication system operates for at least a minute.

3. EXPERIMENTAL RESEARCH PROCEDURE

The research stand for the ICE TCR is designed to determine the actual operating parameters. The research stand is used to test ICE TCRs of various equivalent powers and record their parameters. The full-sized research stand was developed on the basis of the ZMZ-4062 engine with a K27-145 TCR (Fig. 10).

The operating speed range of the K27-145 turbocharger is from 30,000 to 130,000rpm. The turbocharger rotor shaft speed is limited to 75,000rpm for the ZMZ-4062 engine. Taking into account the manufacturer's conditions, the operating range of the K27-145 turbocharger was taken from 0 to 75,000rpm.

The research stand consists of a frame, a hydraulic system, an electrical system, instruments and controls, measuring devices, hydraulic fittings, and mechanical connections.

The frame is installed with a 2,260 cm^3 4-cylinder, 16-valve ZMZ-4062 engine with 1-2-4-3 operating order of cylinders and a microprocessor control system. The ZMZ-4062 engine was started by a 5.5 kW electric motor through a belt drive and a 4-speed GAZ-52 transmission with the ability of motoring at the engine crankshaft speed.

Fig. 10. The research stand based on the ZMZ-4062 engine with a K27-145 TCR.

The use of the GAZ-52 transmission (with fixed gear ratios) allows us to minimize the influence of inertia and stabilize the engine speed. Subsequently, to load the ICE (and thereby reach the operating parameters), a NSh-73 pump was connected to the output shaft of the transmission. The electric motor in the configuration not only exercises starting functions but also acts as a brake, i.e., it allows us to keep the engine speed at a constant level with high accuracy.

When preparing for the experiment, we connected an autonomous oil station to the TCR lubrication system. The oil station allows us to smoothly change the oil supply and pressure on the TCR bearing. The heating elements installed in the tank of the oil station allow us to change the oil temperature at the inlet to the TCR bearing (K27-145). To measure the instantaneous values of the signals, we used USB Autoscope III (Postolovsky Oscilloscope) [34]. A compact APZ 3020 differential pressure sensor was used to control the instantaneous pressure value.

A three-way valve with an oil flow meter at the TCR drain and a thermocouple for measuring the instantaneous oil temperature at the outlet of the TCR bearing is installed under the TCR.

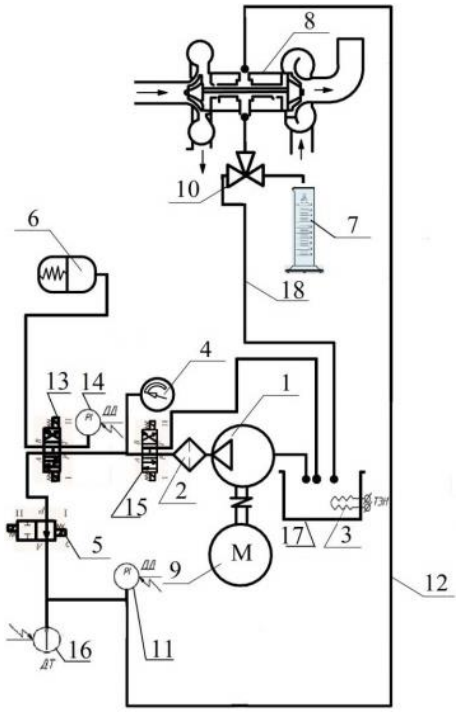

Fig. 11. Scheme of the hydraulic lubrication system of the rig: 1 – oil pump; 2 – oil filter; 3 – thermal electric heater; 4 – oil pressure gauge in the lubrication system of the rig; 5 – distribution valve; 6 – spring hydraulic accumulator; 7 – measuring cup; 8 – turbocharger; 9 – electric motor; 10 – three-way valve; 11, 14 – pressure sensors; 12 – pressure line; 13 – distribution manifold; 15 – distributor; 16 – temperature sensor (thermocouple); 17 – hydraulic tank; 18 – drain line.

The hydraulic system is meant to provide lubrication and cooling of the TCR bearings during operation, as well as to charge the hydraulic accumulator and provide lubrication and cooling of the TCR bearings when the regular lubrication system is inoperable and the TCR operates in the rotor rundown mode (Fig. 11).

The hydraulic system of the rig consists of an 8-liter hydraulic tank 17 with filler and drain plugs, as well as a built-in heating element (thermal electric heater) 3 used to heat oil. A geared oil pump 1 with a variable capacity (1–5l/min) is connected to the hydraulic tank 17 using a copper pipeline. The pump is driven by an asynchronous 0.75kW electric motor 9. An oil filter 2 is connected to the pressure line of the pump, as well as to an electric hydraulic distributor (PX 06574A1) by its outlet pipeline. The distributor 15 is connected to the hydraulic tank (to drain) and a distribution manifold 13 by its outlets via copper pipelines. A distribution manifold 13 is connected to an

electric hydraulic distributor 5, a pressure sensor (PS) 14, and a hydraulic accumulator 6 by its discharge cavities. The hydraulic distributor 5 is connected to the TCR 27-145 inlet bearing channel with its outlet channel, as well as with the incoming oil temperature sensor (TS) 16 and pressure sensor (DD) 11 through a tee. One outlet of the drain line of the TCR bearing is connected to a hydraulic tank 17, and the other one – to a measuring cup 7 through a three-way valve 10.

The electrical system of the rig is meant to power the electric motor 1 (0.75kW) of the gear pump drive of the lubrication system (Fig. 12). The electric circuit ensures:

- switching of the main systems and testing of the TCR in various operating modes of the internal combustion engine;
- operating simplicity and reliability;
- electrical safety of operation personnel;
- remote switching of various elements and systems;
- overload, short circuit, and error protection.

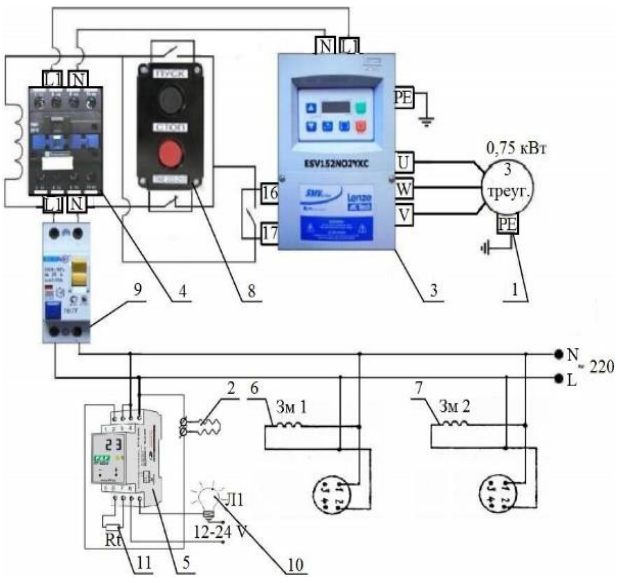

Fig. 12. Electric circuit of the rig: 1 – electric motor; 2 – thermal electric heater; 3 – frequency converter; 4 – magnetic starter; 5 – heat regulator of the thermal electric heater; 6, 7 – electromagnetic coils of hydraulic distributors; 8 – Start-stop buttons; 9 – thermal safety relay; 10 – control lamp of the alarm system; 11 – temperature sensor.

To power the thermal electric heater 2 used to heat oil in the hydraulic tank of the rig, power the frequency converter 3, the starter coils 4, the heat regulator 5 of the thermal electric heater, power the electromagnets of the hydraulic distributors 6 and 7, the Start-Stop buttons, the thermal safety relay 9, the control alarm lamps 10, the temperature sensor 11.

The electrical system of the ICE TCR test rig operates as follows: 22V single-phase alternating current is supplied to the input contacts of the electrical system of the rig. The electromagnetic coils of the hydraulic distributors are connected in parallel with the input contacts to control the operation of the hydraulic distributors at the operator's command. Next, the thermal electric heater 2 is connected in parallel with the heat regulator 5, which provides for the stepless control of the oil temperature in the hydraulic tank. Then, a thermal safety relay is connected in parallel to protect the electric motor of the rig from overheating and overload. A magnetic starter 4 controlled by the Start-stop buttons 8 is connected to the thermal relay; a frequency converter 3 is connected to them to control the speed of the 0.75kW electric motor 1, which winding is connected in a triangle.

In normal operating mode, oil enters the return line and is drained back into the oil tank. However, when it is necessary to estimate the oil flow through the TCR bearing, the valve switches to a special line and a container is used to measure the oil flow through the bearing at a given temperature. In our research, we used a fillable container and recorded the time of its filling using a stopwatch. After that, the valve was switched back and the oil was again supplied to the oil tank. We also measured the instantaneous air consumption, hourly fuel consumption, and specific cycle fuel consumption using an MT-10 motor tester [35].

A full factorial experiment design (FFE 2^3) was chosen. Two factors and one or several effective features are selected (in our case, this is the rundown time of the TCR rotor). The number of experiments in our case with three variation intervals is 8. The final design of the experiment is a combination of eight rows, including a triple combination of factors and eight columns. When calculating the regression equations, we used a nonlinear regression since the mutual influence of the factors has obvious

breaks, maximums and minimums. The experimental data were processed using the SIGMAPLOT application.

4. RESULTS OF EXPERIMENTAL STUDIES AND THEIR ANALYSIS

4.1. The dependence of T_{in} on P_{in} and n at different oil temperatures at the inlet to the TCR bearing (T_{out})

The oil temperature at the TCR drain (Fig. 13) depends equally on the value of the inlet pressure and the TCR rotor speed.

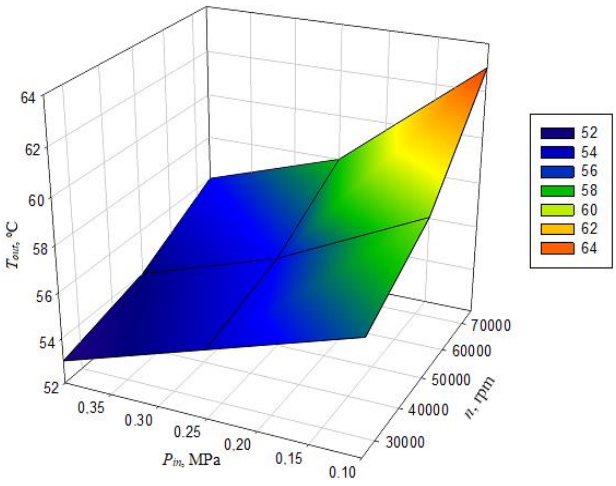

Fig. 13. The dependence of the oil temperature at the TCR drain on the inlet pressure and the TCR rotor speed (T_{in}=50 ºC).

A decrease in the oil temperature at the TCR drain (at a TCR rotor speed of 25,000 rpm) with an increase in the inlet pressure from 0.1 to 0.4 MPa was 4 ºC (53–57ºC). In the zone of high speeds (n = 75,000 rpm), the difference was 7ºC (56–63ºC). Heat generation in the zone of high TCR rotor speeds increases markedly. However, an increase in the TCR rotor speed at a constant value of the inlet oil pressure leads to an increase in the oil temperature at the TCR drain (T_{out}). An increase in the TCR rotor speed from 25,000 to 75,000 rpm (with an input pressure of 0.1 MPa) leads to an increase in the oil temperature at the TCR drain of 6ºC (57–63ºC). In the zone of the inlet pressure of 0.4 MPa, the increase in the oil temperature at the TCR drain was 3ºC (53–56ºC). A smaller increase in the oil temperature at the drain is explained by the good oil pumpability at an inlet pressure of 0.4 MPa, while at low inlet pressure, the pumpability drops and the oil outlet temperature increases significantly, more dynamically at high TCR rotor speeds.

The dependence shown in Fig. 13 can be approximated by the following quadratic Eq. (11):

$$T_{out}(n, P_{in}) = 60.8 - 2.66 \cdot 10^{-5} \cdot n - 32.5 \cdot P_{in} + \\ + 1.06 \cdot 10^{-9} \cdot n^2 + 29.6 \cdot P_{in}^2 \quad (11)$$

With an oil temperature at the TCR bearing inlet of 70ºC, we measured the oil temperature at the TCR drain depending on the inlet pressure before the TCR bearing and the TCR rotor speed (Fig. 14).

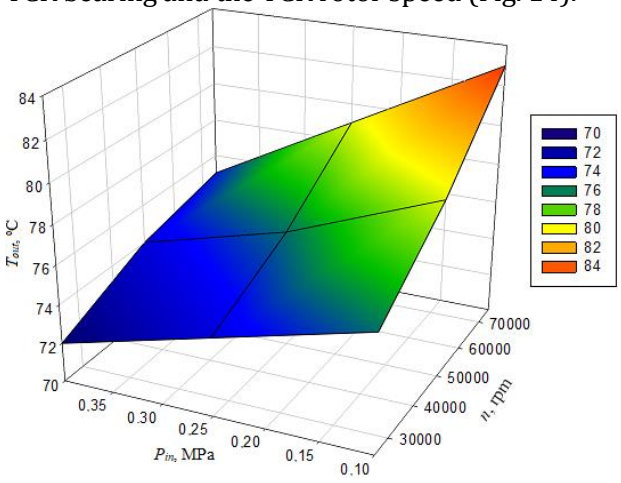

Fig. 14. The dependence of the oil temperature at the TCR drain on the inlet pressure and the TCR rotor speed (T_{in}=70ºC).

The oil temperature at the TCR drain (Fig. 14) depends equally on the value of the inlet pressure and the TCR rotor speed. A decrease in the oil temperature at the TCR drain (at a TCR rotor speed of 25,000 rpm) with an increase in the inlet pressure from 0.1 to 0.4 MPa was 4ºC (72–76ºC). In the zone of high speeds (n=75,000 rpm), the difference was 8ºC (75–83ºC). Heat generation at high TCR rotor speeds increases markedly. However, an increase in the TCR rotor speed at a constant value of the inlet oil pressure leads to an increase in the oil temperature at the TCR drain T_{out}. An increase in the TCR rotor speed from 25,000 to 75,000 rpm (with an input pressure of 0.1 MPa) leads to an increase in the oil temperature at the TCR drain from 76 to 83ºC. In the zone of the inlet pressure of 0.4 MPa, the increase in the oil temperature at the TCR drain was 3ºC (72–75ºC). A smaller increase in the oil temperature at the drain is explained by the good oil pumpability at a high inlet pressure of 0.4 MPa, while at low inlet pressure, the pumpability drops and the oil outlet temperature increases significantly, more dynamically at high TCR rotor speeds.

The dependence shown in Fig. 14 can be approximated by the following quadratic Eq. (12):

$$T_{out}(n, P_{in}) = 70.3 - 5.68 \cdot 10^{-5} \cdot n - 35.5 \cdot P_{in} + \\ + 1.12 \cdot 10^{-9} \cdot n^2 + 79.8 \cdot P_{in}^2 \quad (12)$$

At the oil temperature at the TCR bearing inlet T_{in} =90ºC, we measured the oil temperature at the TCR drain depending on the inlet pressure before the TCR bearing and the TCR rotor speed (Fig. 15).

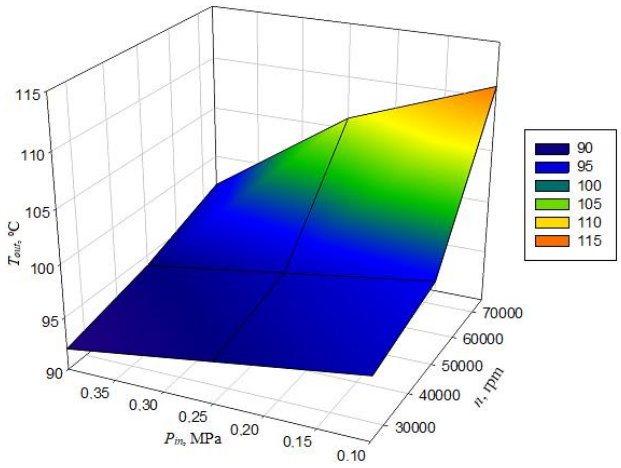

Fig. 15. The dependence of the oil temperature at the TCR drain on the inlet pressure and the TCR rotor speed (T_{in}=90ºC).

The oil temperature at the TCR drain (Fig. 15) depends equally on the inlet pressure and the TCR rotor speed. A decrease in the oil temperature at the TCR drain (at the TCR rotor speed of 25,000 rpm) with an increase in the inlet pressure from 0.1 to 0.4 MPa was 4ºC. In the zone of high speeds (n = 75,000 rpm), the difference was 4ºC. Heat generation in the zone of high TCR rotor speeds increases markedly. However, an increase in the TCR rotor speed at a constant value of the inlet oil pressure leads to an increase in the oil temperature at the TCR drain. An increase in the TCR rotor speed from 25,000 to 75,000 rpm (with an input pressure of 0.1 MPa) leads to an increase in the oil temperature at the TCR drain from 96 to 111ºC. In the zone of the inlet pressure of 0.4 MPa, the increase in the oil temperature at the TCR drain was 5ºC. The smaller increase in the oil temperature at the drain is explained by the good oil pumpability at a high inlet pressure of 0.4 MPa, while at low inlet pressure, the pumpability drops and the oil outlet temperature increases significantly, more dynamically at high TCR rotor speeds.

The dependence shown in Fig. 15 can be approximated by the following quadratic Eq. (13):

$$T_{out}(n, P_{in}) = 103.37 - 0.0003 \cdot n - 9.6 \cdot P_{in} + \\ + 5.33 \cdot 10^{-9} \cdot n^2 - 29.6 \cdot P_{in}^2 \quad (13)$$

4.2. The dependence of T_{out} on T_{in} and n at P_{in}

Fig. 16 shows the oil temperature at the TCR drain depends equally on the oil temperature at the inlet and the TCR rotor speed.

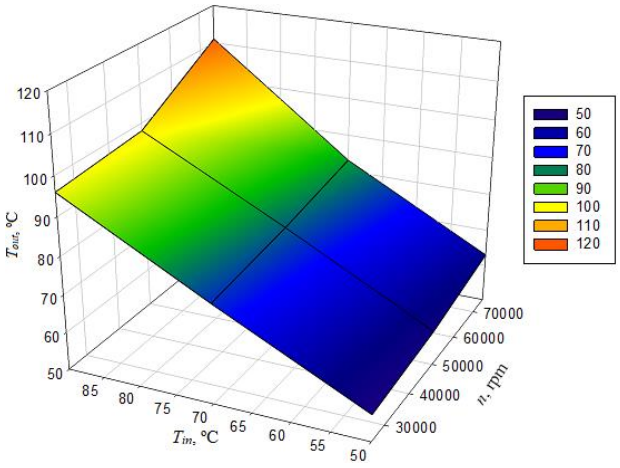

Fig. 16. The dependence of the oil temperature at the TCR drain on the inlet oil temperature to the TCR bearing and the TCR rotor speed with the oil pressure at the inlet to the TCR bearing P_{in}=0.1 MPa.

A decrease in the oil temperature at the TCR drain (with a TCR rotor speed of 25,000 rpm) with an increase in the inlet temperature from 50 to 90 ºC was 39 ºC (57–96ºC). At n = 75,000 rpm, the difference was 48ºC (63–111ºC). Heat generation in the zone of high TCR rotor speeds increases markedly. However, an increase in the TCR rotor speed at a constant temperature of the inlet oil leads to an increase in the oil temperature at the TCR drain. An increase in the TCR rotor speed from 25,000 to 75,000 rpm (the value of the input temperature is 90ºC) leads to an increase in the oil temperature at the TCR drain from 96 to 111ºC. In the zone of the inlet temperature of 50 ºC, the increase in the oil temperature at the TCR drain was 6ºC. The larger increase in oil temperature at the drain at high input oil temperatures is explained by the increased heat transfer from the TCR parts, good oil pumpability at decreased viscosity, while at low inlet temperature, the heat transfer from the TCR parts is orders of magnitude lower.

The dependence shown in Fig. 16 can be approximated by the following quadratic Eq. (14):

$$T_{out}(n,T_{in}) = 20.6 - 0.0002 \cdot n + 0.58 \cdot T_{in} + \\ + 3.73 \cdot 10^{-9} \cdot n^2 + 0.003 \cdot T_{in}^2 \quad (14)$$

Fig. 17 shows the oil temperature at the TCR drain depends equally on the value of the inlet oil temperature and the TCR rotor speed.

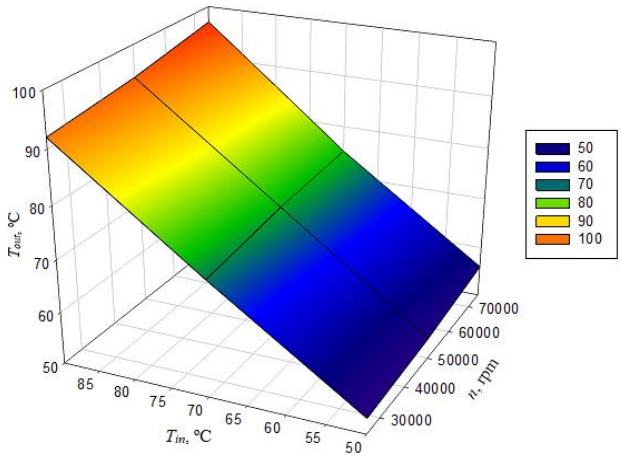

Fig. 17. The dependence of the oil temperature at the TCR drain on the inlet oil temperature to the TCR bearing and the TCR rotor speed with the oil pressure at the inlet to the TCR bearing P_{in}=0.25 MPa.

A decrease in the oil temperature at the TCR drain (with a TCR rotor speed of 25,000 rpm) with an increase in the inlet temperature from 50 to 90ºC was 39ºC. At high speeds (n = 75,000 rpm), the difference was 48ºC. Heat generation at high TCR rotor speeds increases markedly. However, an increase in the TCR rotor speed at a constant inlet oil temperature leads to an increase in the oil temperature at the TCR drain. An increase in the TCR rotor speed from 25,000 to 75,000 rpm (with an input temperature of 90ºC) leads to an increase in the oil temperature at the TCR drain from 94 to 106ºC. With an inlet temperature of 50ºC, the increase in the oil temperature at the TCR drain was 3ºC. The larger increase in the oil temperature at the drain at high input oil temperatures is explained by increased heat transfer from the TCR parts, good oil pumpability with decreased viscosity, while with low inlet temperature, the heat transfer from the TCR parts is orders of magnitude lower.

The dependence shown in Fig. 17 can be approximated by the following quadratic Eq. (15):

$$T_{out}(n,T_{in}) = 15.4 - 0.0001 \cdot n + 0.65 \cdot T_{in} + \\ + 2.66 \cdot 10^{-9} \cdot n^2 + 0.0029 \cdot T_{in}^2 \quad (15)$$

Fig. 18 shows the oil temperature at the TCR drain depends equally on the inlet oil temperature and the TCR rotor speed.

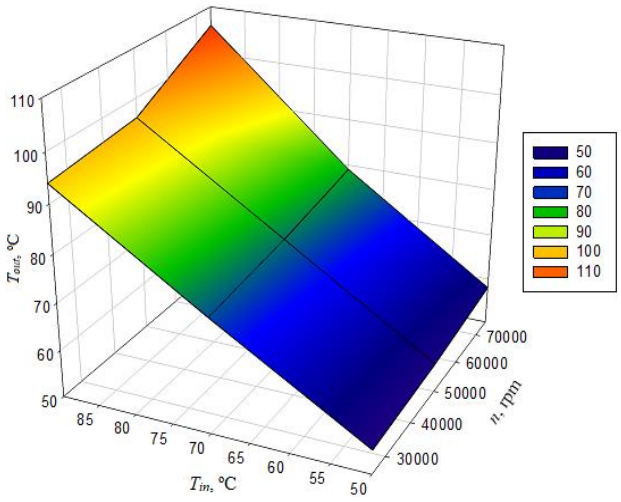

Fig. 18. The dependence of the oil temperature at the TCR drain on the inlet oil temperature to the TCR bearing and the TCR rotor speed with the oil pressure at the inlet to the TCR bearing P_{in}=0.4 MPa

A decrease in the oil temperature at the TCR drain (with a TCR rotor speed of 25,000 rpm) with an increase in the inlet temperature from 50 to 90ºC was 39ºC. In the zone of high speeds (n = 75,000 rpm), the difference was 41ºC. Heat generation at high TCR rotor speeds increases markedly. However, an increase in the TCR rotor speed at a constant value of the inlet oil temperature leads to an increase in the oil temperature at the TCR drain. An increase in the TCR rotor speed from 25,000 to 75,000 rpm (the value of the input temperature is 90ºC) leads to an increase in the oil temperature at the TCR drain from 92 to 97ºC. With an inlet temperature of 50ºC, the increase in the oil temperature at the TCR drain was 3ºC. The larger increase in oil temperature at the drain at high input oil temperatures is explained by an increased heat transfer from the TCR parts, good oil pumpability with decreased viscosity, while with low inlet temperature, the heat transfer from the TCR parts is orders of magnitude lower.

The dependence shown in Fig. 18 can be approximated by the following quadratic Eq. (16):

$$T_{out}(n,T_{in}) = 8.7 + 4.66 \cdot 10^{-5} \cdot n + 0.76 \cdot T_{in} + \\ + 2.66 \cdot 10^{-9} \cdot n^2 + 0.0017 \cdot T_{in}^2 \quad (16)$$

4.3. The dependence of T_{out} on P_{in} and P_{in} at n

The oil temperature at the TCR drain (Fig. 19) insignificantly depends on a change in the input oil pressure. The difference in the inlet pressures of 0.4–0.25 MPa (at T_{in}=50ºC) leads to a slight increase in the oil temperature at the TCR drain (53–55ºC), whereas the difference between the inlet pressures of 0.25–0.1 MPa leads to a slight (linear) increase in the oil temperature at the TCR drain (55–57ºC).

Fig. 19 shows that with an increase in the inlet oil temperature to the TCR bearing, the oil temperature at the TCR drain increases. At a constant inlet oil pressure of 0.4 MPa, an increase in the inlet oil temperature to the TCR bearing within the range 50–90ºC leads to an increase in the oil temperature at the TCR drain from 53 ºC to 92ºC. At an oil pressure of 0.1 MPa, the increase is from 57ºC to 96ºC. At lower pressure, heat transfer is significantly higher, which explains the increase in the oil temperature at the TCR drain.

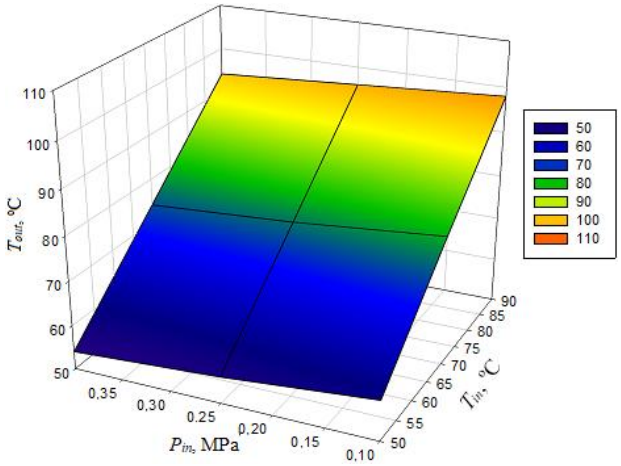

Fig. 19. The dependence of the oil temperature at the TCR drain on the oil pressure and temperature at the inlet to the TCR bearing with a TCR rotor speed of n=25,000 rpm.

The dependence shown in Fig. 19 can be approximated by the following quadratic Eq. (17):

$$T_{out}(P_{in},T_{in}) = 15.2 + 0.8 \cdot T_{in} - 13.3 \cdot P_{in} + \\ + 0.0012 \cdot T_{in}^2 - 2.91 \cdot 10^{-11} \cdot P_{in}^2 \quad (17)$$

The oil temperature at the TCR drain (Fig. 20) insignificantly depends on the change in the input oil pressure. The difference in the inlet pressures of 0.4–0.25 MPa (at T_{in}=50ºC) leads to a slight increase in the oil temperature at the TCR drain (54–56ºC), whereas the difference between the inlet pressures of 0.25–0.1 MPa leads to a slight (almost linear) increase in the oil temperature at the TCR drain (56–59ºC). Fig. 20 shows that with an increase in the inlet oil temperature to the TCR bearing, the oil temperature at the TCR drain increases. At a constant inlet oil pressure of 0.4 MPa, an increase in the inlet oil temperature to the TCR bearing from 50 to 90ºC leads to an increase in the oil temperature at the TCR drain from 54 ºC to 94ºC. At an oil pressure of 0.1 MPa, the increase is from 59 ºC to 98ºC. At lower pressure, heat transfer is significantly higher, which explains the increase in oil temperature at the TCR drain.

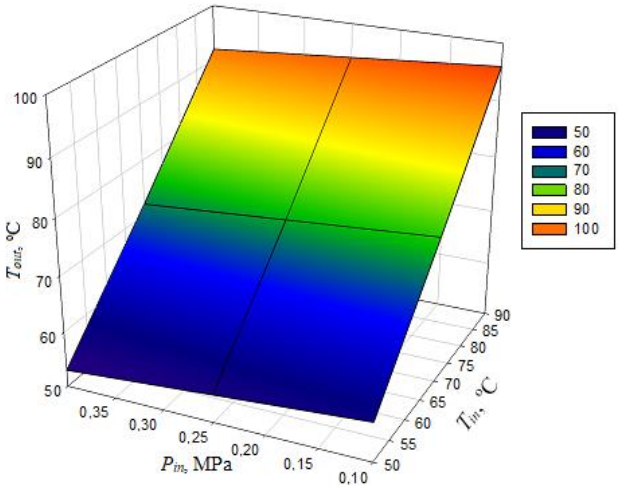

Fig. 20. The dependence of the oil temperature at the TCR drain on the oil pressure and temperature at the inlet to the TCR bearing with a TCR rotor speed of n=50,000 rpm.

The dependence shown in Fig. 20 can be approximated by the following quadratic Eq. (18):

$$T_{out}(P_{in},T_{in}) = 9.46 + 1.05 \cdot T_{in} - 22.9 \cdot P_{in} + \\ + 0.0004 \cdot T_{in}^2 + 14.81 \cdot P_{in}^2 \quad (18)$$

The oil temperature at the TCR drain (Fig. 21) insignificantly depends on the change in the input oil pressure. A difference in the inlet pressures of 0.4–0.25 MPa (at T_{in}=50ºC) leads to a slight increase in the oil temperature at the TCR drain (56–58ºC), whereas the difference between the inlet pressures of 0.25–0.1 MPa leads to an imperceptible (almost linear) increase in the oil temperature at the TCR drain (58–63ºC).

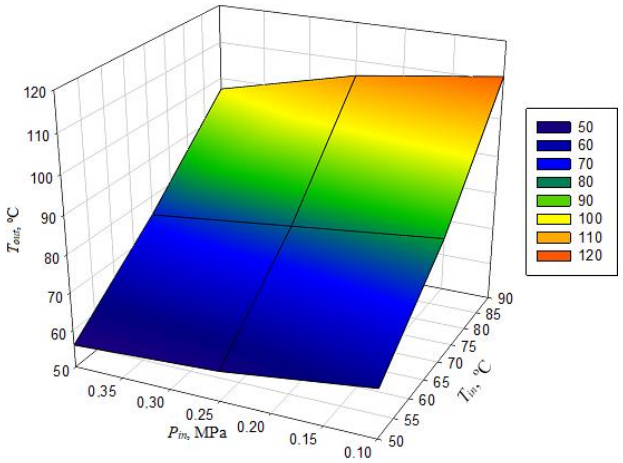

Fig. 21. The dependence of the oil temperature at the TCR drain on the oil pressure and temperature at the inlet to the TCR bearing with a TCR rotor speed of n=75,000 rpm.

Fig. 21 shows that with an increase in the inlet oil temperature to the TCR bearing, the oil temperature at the TCR drain increases. With a constant value of the inlet oil pressure of 0.4 MPa, an increase in the inlet oil temperature to the TCR bearing within from 50 to 90ºC leads to an increase in the oil temperature at the TCR drain from 56ºC to 97ºC. With an oil pressure of 0.1 MPa, the increase is from 63ºC to 111ºC. At lower pressure, heat transfer is significantly higher, which explains the increase in oil temperature at the TCR drain. The dependence shown in Fig. 21 can be approximated by the following quadratic Eq. (19):

$$T_{out}\left(P_{in},T_{in}\right)=41.49+0.15\cdot T_{in}-28.5P_{in}+ \\ +0.007\cdot T_{in}^{2}+7.4\cdot P_{in}^{2} \quad (19)$$

5. CONCLUSION

The TCR accounts for 7% to 27% of failures. Failures mainly occur due to a lack of lubrication, low pressure, or an excessive temperature rise. When operating TCRs, it is essential to maintain the thermal balance in all possible ICE operating modes. The worst modes of lubricating the TCR bearing are the stop and start modes. However, the stop mode is most extreme, when the oil temperature in the bearing clearance can exceed the flash point and cause oil coking in the TCR working clearances and channels. The main reasons for the malfunctioning of a turbocharged ICE are high dynamic loads, significant thermal loads in friction zones, wear of the TCR elements, the overheating of components and systems, and oil starvation. A comprehensive analysis allowed us to establish the most effective way to extend the service life of an ICE with a TCR by using a hydraulic accumulator with an independent lubrication system. Violations of the standard operating modes of the TCR, which are often random and occur suddenly. The violation of normal modes can be excluded if we study the operating parameters with the output indicators of the TCR operation. The installation of a hydraulic accumulator in the lubrication system, which continuously maintains the liquid friction mode in the clearance and a favorable rundown of the TCR rotor, provides the necessary conditions for the lubrication of the TCR. The main conclusions are:

1. We proposed to use an adaptive external independent lubrication system to feed the bearings of modern turbochargers;
2. We established theoretically that the maximum temperature of the TCR bearing can reach 260ºC at the 200th second after the ICE stops, which is in the flash point zone of modern oils and is dangerous by coking of the inner oil layers in the TCR bearing clearance and its channels;
3. We established theoretically that at exhaust gas temperature t_{ex}=600ºC and the minimum operating time of the autonomous lubrication system, the temperature $t_{bearing}$ reaches a maximum value of about 210ºC.
4. We developed a test rig to test the turbocharger in the operating range of the input and output parameters of its operation process;
5. We developed an autonomous lubrication system allowing us to set independently the oil pressure range before the bearing from 0 to 0.5MPa, the oil temperature up to 130ºC, as well as the oil flow through the bearing when setting any input pressure and oil temperature.
6. We checked experimentally and set the operability limits of the turbocharger lubrication system within the operating speed range of the turbocharger rotor shaft;
7. We established experimentally an increase in the oil temperature at the TCR drain to 111ºC at an oil temperature at the input to the TCR bearing T_{in}=90ºC in the high speed zone n=75,000rpm.

REFERENCES

[1] I.G. Galiev, A.T. Kulakov, A.R. Galimov, *Individual lubrication system for the internal combustion engine turbocharger bearing assembly*, Proceedings of the Crimean Engineering and Pedagogical University, vol. 2, no. 68, pp. 252–258, 2020. (in Russian)

[2] A.V. Gritsenko, A.M. Plaksin, A.Yu. Burtsev, *Studying the rundown of the TKR-11 turbocharger rotor*, Agrofood Policy of Russia, vol. 1, no. 37, pp. 52–55, 2015. (in Russian)

[3] V. Shepelev, A. Gritsenko, G. Salimonenko, *Control of hydrocarbon emissions when changing the technical condition of the exhaust system of modern cars*, FME Transactions, vol. 49, no. 3, pp, 749–755, 2021, doi: 10.5937/fme2103749S

[4] A. Pagot, A. Duparchy, X. Gautrot, P. Leduc, G. Monnier, *Combustion approach for downsizing: The IFP concept*, Oil & Gas Science and Technology – Rev. IFP, vol. 61, no. 1, pp 139–153, 2006, doi: 10.2516/ogst:2006009x

[5] P. Dellis, R. Evaggelos, G. Alcibiades, A. Pesyridis, *Turbocharger lubrication -lubricant behavior and factors that cause turbocharger failure*, International Journal of Automotive Engineering and Technologies, vol. 2, iss. 1, pp. 40–54, 2013.

[6] W.J. Chen, *Rotor dynamics and bearing design of turbochargers*, Mechanical Systems and Signal Processing, vol. 29, pp. 77–89, 2012, doi: 10.1016/j.ymssp.2011.07.025

[7] A. Gritsenko, V. Shepelev, S. Fedoseev, T. Bedych, *Increase in the fuel efficiency of a diesel engine by disconnecting some of its cylinders*, Facta Universitatis. Series: Mechanical Engineering, Online first, 2022, doi: 10.22190/FUME210914002G

[8] J. Galindo, A. Tiseira, R., Navarro, D. Tarí, C.M., Meano, *Effect of the inlet geometry on performance, surge margin and noise emission of an automotive turbocharger compressor*, Applied Thermal Engineering, vol. 110, pp. 875–882, 2017, doi: 10.1016/j.applthermaleng.2016.08.099

[9] A.V. Gritsenko, V.D. Shepelev, I.V. Makarova, *Diagnostics of the fuel supply system of auto ICEs by the test method*, Journal of King Saud University - Engineering Science, In Press, 2021, doi: 10.1016/j.jksues.2021.03.008

[10] H.C. Kuhn, R. da Rosa Righi, C.D.P. Crovato, *On proposing a non-intrusive device and methodology to monitor motor degradation*, Journal of King Saud University - Engineering Science, In Press, 2021, doi: 10.1016/j.jksues.2021.04.007

[11] D.Y. Dhande, D.W. Pande, *Multiphase flow analysis of hydrodynamic journal bearing using CFD coupled Fluid Structure Interaction considering cavitation*, Journal of King Saud University - Engineering Science, vol. 30, iss. 4, pp. 345–354, 2018, doi: 10.1016/j.jksues.2016.09.001

[12] A.V. Gritsenko, E.A. Zadorozhnaya, V.D. Shepelev, *Diagnostics of friction bearings by oil pressure parameters during cycle-by-cycle loading*, Tribology in Industry, vol. 40, no. 2, pp. 300–310, 2018, doi: 10.24874/ti.2018.40.02.13

[13] S.S. Alaviyoun, M. Ziabasharhagh, *Experimental thermal survey of automotive turbocharger*, International Journal of Engine Research, vol. 21, iss. 5, pp. 766–780, 2020, doi: 10.1177/1468087418778987

[14] H. Basir, A. Gharehghani, A. Ahmadi, S.M. Agha Mirsalim, M.A. Rosen, *Experimental and numerical investigation on the heat transfer of an automotive engine's turbocharger,* Proceedings of the Institution of Mechanical Engineers, Part D: Journal of Automobile Engineering, vol. 235, iss. 8, pp. 2124–2135, 2021, doi: 10.1177/0954407020987829

[15] R. Taylor, H. Hu, C. Stow, T. Davenport, R Mainwaring., S. Rappaport, S. Remmert, *Extending the Limits of Fuel Economy through Lubrication*, SAE Technical Papers, 2017, doi: 10.4271/2017-01-2344

[16] P.S. Dellis, *Piston-ring performance: limitations from cavitation and friction,* International Journal of Structural Integrity, vol. 10, iss. 3, pp. 304–324, 2019, doi: 10.1108/IJSI-09-2018-0053

[17] P.S. Dellis, *Piston ring performance II: measurement of cavitation shapes in different operating conditions and their link to lubricant properties*, International Journal of Structural Integrity, vol. 13, iss. 4, pp. 611 – 631, 2022, doi: 10.1108/IJSI-09-2021-0095

[18] A. Gil, A.O. Tiseira, L.M. García-Cuevas, T.R. Usaquén, G. Mijotte, *Fast three-dimensional heat transfer model for computing internal temperatures in the bearing housing of automotive turbochargers*, International Journal of Engine Research, vol. 21, iss. 8, pp. 1286–1297, 2020, doi: 10.1177/1468087418804949

[19] J.R. Serrano, A.O.T. Izaguirre, L.M. García-Cuevas, T.R. Usaquén, M. Guillaume, *A methodology to study oil-coking problem in small turbochargers*. International Journal of Engine Research, vol. 21, iss. 7, pp. 1193–1204, 2020, doi: 10.1177/1468087418803197

[20] J.R. Serrano, A. Tiseira, L.M. García-Cuevas, T.R. Usaquén, *Adaptation of a 1-D tool to study transient thermal in turbocharger bearing housing*, Applied Thermal Engineering, vol. 134, pp. 564–575, 2018, doi: 10.1016/j.applthermaleng.2018.01.085

[21] P. Podevin, A. Clenci, G. Descombes, *Influence of the lubricating oil pressure and temperature on the performance at low speeds of a centrifugal compressor for an automotive engine*, Applied Thermal Engineering, vol. 31, no. 2-3, pp. 194–201, 2011, doi: 10.1016/j.applthermaleng.2010.08.033

[22] O.R. Sandoval, L.H. Machado, B. Caetano, I.F. Lara, R. Molina, *Influence of temperature and injection pressure of lubrication in the vibration of an automotive turbocharger,* Mechanisms and Machine Science, vol. 63, pp. 388–397, 2019, doi: 10.1007/978-3-319-99272-3_27

[23] D. Hadryś, H. Bąkowski, Z. Stanik, A. Kubik, *Analysis of shaft wear in turbocharges of automotive vehicles*, Transport Problems, vol.14, no. 3, pp. 85–95, 2019, doi: 10.20858/tp.2019.14.3.8

[24] P. Novotný, J. Vacula, J. Hrabovský, *Solution strategy for increasing the efficiency of turbochargers by reducing energy losses in the lubrication system,* Energy, vol. 236, 2021, doi: 10.1016/j.energy.2021.121402

[25] S. Chuepeng, S. Saipom, *Lubricant thermo-viscosity effects on turbocharger performance at low engine load*, Applied Thermal Engineering, vol. 139, pp. 334–340, 2018, doi: 10.1016/j.applthermaleng.2018.05.002

[26] P. Novotný, M. Jonák, J. Vacula, *Evolutionary Optimisation of the Thrust Bearing Considering Multiple Operating Conditions in Turbomachinery,* International Journal of Mechanical Sciences, vol. 195, 2021, doi: 10.1016/j.ijmecsci.2020.106240

[27] R.R. Mutra, J. Srinivas, R. Rządkowski, *An optimal parameter identification approach in foil bearing supported high-speed turbocharger rotor system,* Archive of Applied Mechanics, vol. 91, iss. 4, pp. 1557–1575, 2021, doi: 10.1007/s00419-020-01840-x

[28] R.R. Mutra, J. Srinivas, R., *Dynamic Analysis of a Turbocharger Rotor-Bearing System in Transient Operating Regimes*, Journal of The Institution of Engineers (India): Series C, vol. 101, iss. 5, pp. 771–783, 2020, doi: 10.1007/s40032-020-00591-6

[29] R.R. Mutra, J. Srinivas, R. *An optimization-based identification study of cylindrical floating ring journal bearing system in automotive turbochargers,* Meccanica, vol. 57, iss. 5, pp. 1193 – 1211, 2022, doi: 10.1007/s11012-022-01507-7

[30] A. Gritsenko, E. Zadorozhnaya, V. Shepelev, I. Gimaltdinov, *Parameters of internal combustion engine efficiency while introducing additives in the oil*, Tribology in Industry, vol. 41, no.4, pp. 592–603, 2019, doi: 10.24874/ti.2019.41.04.11

[31] A. R. Galimov, I. G. Galiev, K. A. Khafizov, E. R. Galimov, *Determining and ensuring the turbocharger operability*, Bulletin of NGIEI, vol.4, no. 119, pp. 42–50, 2021. (in Russian)

[32] A. S. Denisov, A. A. Korkin, A. R. Asoyan, *Analysis of factors affecting the performance of the turbocharger bearing assembly*, Bulletin of the Saratov State Technical University, vol. 3, no. 46, pp. 53–57, 2010. (in Russian)

[33] D. Ya. Nosyrev, A. A. Svechnikov, Yu. Yu. Stanovova, *Experimental studies of the operation of a turbocharger at the moment of the beginning of rotation and at the moment of stopping*, Bulletin of transport of the Volga region, vol. 1, no. 43, pp. 15–19, 2014.

[34] USB Autoscope III Operation Manual, available at: http://www.autoscaners.ru/catalogue/files/689/program_usb_oscilloscope.pdf

[35] Motor-Tester MT10KM computer diagnostic complex, available at: http://www.nppnts.com/index.php?mod=mtmt10km